Physics Letters B 318 (1993) 347–353
North-Holland

PHYSICS LETTERS B

SUSY Higgs production at proton colliders

M. Spira [a], A. Djouadi [b,1], D. Graudenz [c,2] and P.M. Zerwas [a]

[a] *Deutsches Elektronensynchrotron DESY, D-22603 Hamburg, FRG*
[b] *Lab. de Physique Nucléaire, Univ. de Montréal, H3C 3J7 Montréal, Canada*
[c] *Lawrence Berkeley Laboratory, Univ. of California, Berkeley, CA 94720, USA*

Received 4 October 1993
Editor: P.V. Landshoff

We present the QCD corrections to the gluon fusion processes of the scalar Higgs particles h, H and the pseudoscalar Higgs particle A in the minimal supersymmetric extension of the Standard Model. These corrections are in general large and positive, increasing the production cross section up to factors of about 2. While they depend only weakly on the Higgs masses, they are strongly dependent on the parameter $\mathrm{tg}\,\beta$.

Supersymmetric theories provide well-motivated scenarios for electroweak symmetry breaking [1]. These theories do not suffer from the naturalness (or hierarchy) problem of the Standard Model, and they can be extended up to the GUT scale while retaining the Higgs bosons as light elementary particles. In contrast to the Standard Model [SM], supersymmetric theories incorporate a spectrum of several Higgs particles. Five scalar states [#1] are realized in the minimal version of the supersymmetric extension of the Standard Model [MSSM], one light and one heavy scalar particle h, H [CP-even], a pseudoscalar particle A [CP-odd], and a pair of charged Higgs particles. While the mass of the light scalar particle h is bounded – on general theoretical grounds – to be less than 150 GeV, the masses of the other particles are expected to be of the order of the electroweak symmetry breaking scale, i.e. below $\sim$ 1 TeV.

The dominant production mechanism for the neutral Higgs bosons h, H and A at proton–proton colliders is gluon–gluon fusion [2]. The Higgs bosons couple to the gluons primarily through heavy quark t, b triangle loops. In this note we present the QCD corrections to the cross sections $\sigma(pp \to h/H/A + X)$ of these processes,

$$gg \to \Phi(g) \quad \text{and} \quad gq \to \Phi q, \quad q\bar{q} \to \Phi g. \tag{1}$$

Generic diagrams of these subprocesses are depicted in fig. 1. The proper control of these corrections is demanded by the fact that rare $\gamma\gamma$ and $\tau^+\tau^-$ decays provide most important experimental channels to detect these particles at proton colliders so that the precise knowledge of the production cross sections is crucial regarding the small number of events in these channels. This analysis extends previous work on Higgs production in the Standard Model [3] and preliminary studies in the limit of large loop quark masses [4–6]. The QCD corrections to the $\gamma\gamma$ branching ratios of the Higgs particles have been calculated in ref. [5], in conjunction with earlier studies of the $b\bar{b}$ decay widths [7].

Top and bottom quark loops build up the dominant contributions to the couplings of Higgs bosons to gluons. To lowest order (LO), the cross sections for the production of Higgs particles in pp collisions are given by

$$\sigma_{\mathrm{LO}}(pp \to \Phi + X) = \sigma_0^{\Phi}\, \tau_{\Phi} \frac{\mathrm{d}\mathcal{L}^{gg}}{\mathrm{d}\tau_{\Phi}}, \tag{2}$$

where $\mathrm{d}\mathcal{L}^{gg}/\mathrm{d}\tau_{\Phi}$ denotes the gluon luminosity at $\tau_{\Phi} = m_{\Phi}^2/s$ with $\sqrt{s}$ being the c.m. energy of the

[1] NSERC Fellow.
[2] Fellow of Max Kade Foundation (New York).
[#1] The neutral Higgs particles will generically be denoted by Φ.

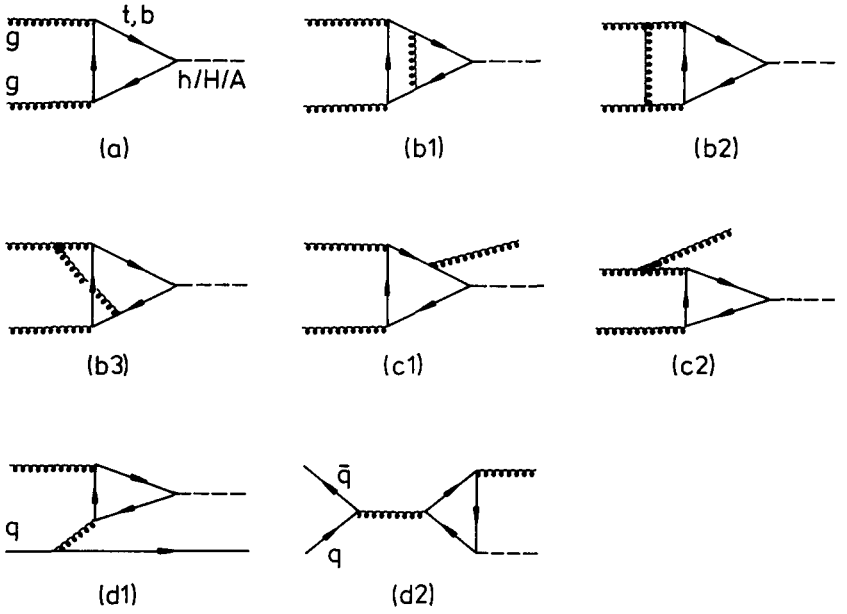

Fig. 1. Generic diagrams of the subprocesses for the production of Higgs particles at pp colliders: (a) lowest-order gg contribution; (b) virtual corrections; (c) real gluon radiation; (d) Higgs production in gq and $q\bar{q}$ collisions.

proton collider. The parton cross sections can be expressed in terms of scalar/pseudoscalar form factors derived from the quark triangle diagrams in fig. 1a,

$$\sigma_0^{h/H} = \frac{G_F \alpha_s^2}{288\sqrt{2}\pi} \left| \sum_Q F_Q^{h/H}(\tau_Q) \right|^2 ,$$

$$\sigma_0^A = \frac{G_F \alpha_s^2}{128\sqrt{2}\pi} \left| \sum_Q F_Q^A(\tau_Q) \right|^2 . \qquad (3)$$

The form factors are related to the scalar triangle integral f,

$$f(\tau_Q) = \begin{cases} \arcsin^2 \sqrt{\tau_Q}, & \tau_Q < 1, \\ -\frac{1}{4}\left[\log \dfrac{1+\sqrt{1-\tau_Q^{-1}}}{1-\sqrt{1-\tau_Q^{-1}}} - i\pi \right]^2, & \tau_Q > 1, \end{cases}$$

in the following way:

$$F_Q^{h/H}(\tau_Q) = \tfrac{3}{2}\tau_Q^{-1}\left[1 + (1-\tau_Q^{-1}) f(\tau_Q)\right] g_Q^{h/H},$$

$$F_Q^A(\tau_Q) = \tau_Q^{-1} f(\tau_Q) g_Q^A, \qquad (4)$$

Table 1
The coefficients of the Higgs couplings to t, b quarks in the MSSM. α, β are mixing angles, with $\mathrm{tg}\,\beta = v_2/v_1$ being the ratio of the Higgs vacuum expectation values; α is given by the masses and $\mathrm{tg}\,\beta$. Numerical values of the coefficients are presented in ref. [8], for instance.

Φ	g_t^Φ	g_b^Φ
h	$\cos\alpha/\sin\beta$	$-\sin\alpha/\cos\beta$
H	$\sin\alpha/\sin\beta$	$\cos\alpha/\cos\beta$
A	$1/\mathrm{tg}\,\beta$	$\mathrm{tg}\,\beta$

with $\tau_Q = m_\Phi^2/4m_Q^2$. The coefficients g_Q^Φ denote the couplings of the Higgs bosons normalized to the SM Higgs couplings to top and bottom quarks; they are recollected for the sake of convenience in table 1. The parameter $\mathrm{tg}\,\beta$ is generally assumed to vary between unity and $\sim m_t/m_b$. The leading radiative corrections are taken into account for the Higgs masses and couplings.

For small values $\mathrm{tg}\,\beta \sim 1$, the t couplings are dominant while b couplings are large for large $\mathrm{tg}\,\beta$. The form factors are normalized such that for

$m_Q \gg m_\Phi$: $F_Q^\Phi \to g_Q^\Phi$,

$m_Q \ll m_\Phi$:

$$F_Q^{h/H} \to 6\frac{m_Q^2}{m_{h/H}^2}\left[1-\frac{1}{4}\left(\log\frac{m_{h/H}^2}{m_Q^2}-i\pi\right)^2\right] g_Q^{h/H},$$

$$F_Q^A \to -\frac{m_Q^2}{m_A^2}\left(\log\frac{m_A^2}{m_Q^2}-i\pi\right)^2 g_Q^A.$$

Both form factors approach zero in the chiral limit $m_Q \to 0$. The leading logarithmic terms also give rise to the same cross section in the scalar and pseudoscalar case in the approach to the chiral limit.

Characteristic diagrams of the QCD radiative corrections are shown in figs. 1b to 1d. They consist of two-loop gluon–quark and Higgs–quark vertex corrections, rescattering corrections and non-planar diagrams. The renormalization program has been carried out in the $\overline{\text{MS}}$ scheme. The "physical" quark mass m_Q is defined at the pole of the propagator; this assures the correct [perturbative] threshold behavior of the triangle amplitude for $m_\Phi \approx 2m_Q$ [4]. The renormalization of the scalar $hQ\overline{Q}$ and $HQ\overline{Q}$ vertices is connected with the renormalization of the quark mass and the quark wave-function, $Z_{hQQ} = Z_Q - \delta m_Q/m_Q$ etc. [7]. For the 't Hooft–Veltman implementation of γ_5 in the dimensional regularization scheme [9] adopted in the present calculation, the renormalization Z_{AQQ} of the pseudoscalar $AQ\overline{Q}$ vertex must be supplemented by an additional term $8\alpha_s/(3\pi)$ to restore chiral invariance in the limit $m_Q \to 0$ and the correct form of the Adler–Bell–Jackiw anomaly [10]. In addition to these virtual corrections, the gluon radiation off the initial state gluons and the heavy quark lines must be taken into account. After adding up all these contributions, ultraviolet and infrared singularities cancel. Leftover collinear singularities are absorbed into the renormalized parton densities [11] which we define in the $\overline{\text{MS}}$ scheme. Finally the subprocesses $gq \to Hq$ and $q\overline{q} \to Hg$ must be added, fig. 1d.

The results for the cross sections can be summarized in the following form:

$$\sigma(pp \to \Phi + X) = \sigma_0^\Phi\left(1 + C^\Phi\frac{\alpha_s}{\pi}\right)\tau_\Phi\frac{d\mathcal{L}^{gg}}{d\tau_\Phi} + \Delta\sigma_{gg}^\Phi + \Delta\sigma_{gq}^\Phi + \Delta\sigma_{q\overline{q}}^\Phi \quad (5)$$

The coefficients C^Φ denote the contributions from the virtual two-loop quark corrections regularized by the infrared singular part of the cross section for real gluon emission,

$$C^\Phi = \pi^2 + c^\Phi + \frac{33-2N_f}{6}\log\frac{\mu^2}{m_\Phi^2},$$

$$c^\Phi = \text{Re}\sum_Q F_Q^\Phi\, c_Q^\Phi(\tau_Q)\Big/\sum_Q F_Q^\Phi. \quad (6)$$

These coefficients split into the infrared term π^2, a term depending on the renormalization scale μ of the coupling constant, and pieces c^Φ which depend on the mass ratios τ_Q, averaged with proper weights over top and bottom loops. The coefficients $c_Q^\Phi(\tau_Q)$ have been reduced from 5-dimensional Feynman parameter integrals to 1-dimensional integrals analytically. The remaining integration has been performed numerically; it has been checked carefully that the results are stable up to values of order $\tau_b \sim 10^4$ corresponding to Higgs masses of order 1 TeV for a bottom mass of 5 GeV. In the limit of large quark masses, these coefficients can be calculated analytically [4–6],

$m_Q \gg m_\Phi$: $c_Q^{h/H} \to \frac{11}{2}$, $c_Q^A \to 6$

For large Higgs masses but moderate quark masses the real and imaginary parts of c_Q^Φ remain small, $\leqslant \pm 5$ for $\tau_Q \leqslant 10^4$. However, the numerical results clearly indicate the onset of the asymptotic behavior $\text{Im}\, c_Q^\Phi \sim \log\tau_Q$ and suggest $\text{Re}\, c_Q^\Phi \sim \log^2\tau_Q$ for large $\log\tau_Q$ [12]. Similarly to the LO form factors, the leading terms appear to approach a common value for h, H and A.

The (non-singular) contributions from gluon radiation in gg scattering, from gq scattering, and $q\overline{q}$ annihilation, figs. 1c, 1d, depend on the renormalization scale μ and the factorization scale M of the parton densities,

$$\Delta\sigma_{gg}^\Phi = \int_{\tau_\Phi}^1 d\tau\frac{d\mathcal{L}^{gg}}{d\tau}\frac{\alpha_s}{\pi}\sigma_0^\Phi\Big\{-zP_{gg}(z)\log\frac{M^2}{\tau s} + d_{gg}^\Phi(z,\tau_Q) + 12\Big[\Big(\frac{\log(1-z)}{1-z}\Big)_+ - z\,[2-z(1-z)]\log(1-z)\Big]\Big\}, \quad (7)$$

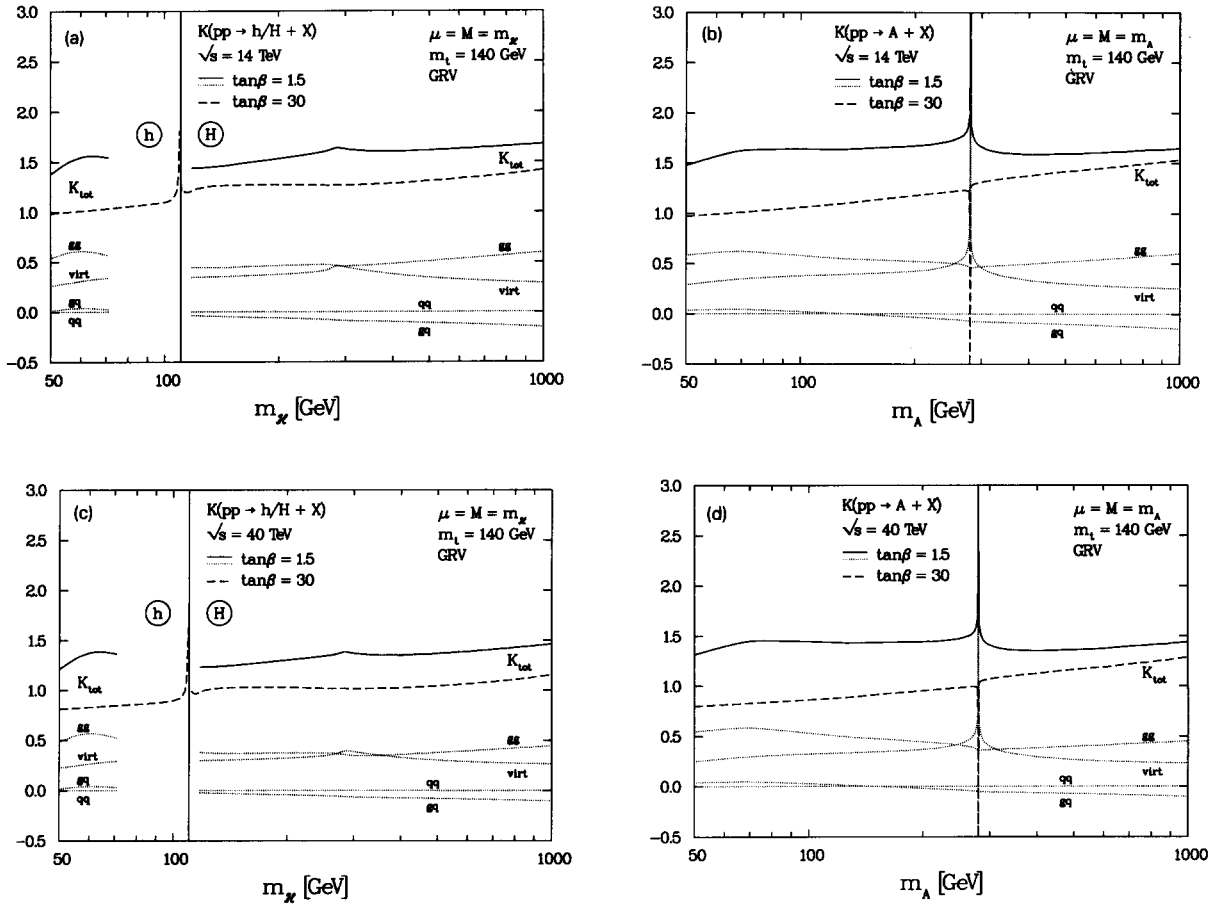

Fig. 2. K factors of the QCD corrected cross sections $\sigma(pp \to h/H/A)$ for two values $\mathrm{tg}\,\beta = 1.5$ and 30. For $\mathrm{tg}\,\beta = 1.5$ the K factor is broken down to its individual contributions (the relative ratios for $\mathrm{tg}\,\beta = 30$ are similar); K_{virt}, regularized virtual contributions; K_{AB}, real corrections $(A, B = q, g)$; K_{tot}, ratios of the QCD corrected cross sections in next-to-leading order to the lowest-order cross sections. For LHC with $\sqrt{s} = 14$ TeV and SSC with $\sqrt{s} = 40$ TeV pp c.m. energies.

$$\Delta\sigma_{gq}^{\Phi} = \int_{\tau_\Phi}^{1} \mathrm{d}\tau \sum_{q,\bar{q}} \frac{\mathrm{d}\mathcal{L}^{gq}}{\mathrm{d}\tau} \frac{\alpha_s}{\pi} \sigma_0^{\Phi} \left\{ \left[-\tfrac{1}{2} \log \frac{M^2}{\tau s} + \log(1-z) \right] z P_{gq}(z) + d_{gq}^{\Phi}(z, \tau_Q) \right\},$$

$$\Delta\sigma_{q\bar{q}}^{\Phi} = \int_{\tau_\Phi}^{1} \mathrm{d}\tau \sum_{q} \frac{\mathrm{d}\mathcal{L}^{q\bar{q}}}{\mathrm{d}\tau} \frac{\alpha_s}{\pi} \sigma_0^{\Phi} d_{q\bar{q}}^{\Phi}(z, \tau_Q), \quad \text{(7 cont'd)}$$

with $z = \tau_\Phi/\tau$ and P_{ij} being the standard Altarelli–Parisi splitting functions. Again, the coefficients $d_{gg}^{\Phi}, d_{gq}^{\Phi}$ and $d_{q\bar{q}}^{\Phi}$, superpositions of properly weighted t- and b-loop contributions, have been reduced to 1-dimensional integrals which have been evaluated numerically. In the limit of large quark masses, the coefficients can be determined analytically [4–6]; they coincide for scalar and pseudoscalar Higgs particles,

$m_Q \gg m_\Phi$:

$$d_{gg}^{\Phi} \to -\tfrac{11}{2}(1-z)^3,$$

$$d_{gq}^{\Phi} \to -1 + 2z - \tfrac{1}{3}z^2,$$

$$d_{q\bar{q}}^{\Phi} \to \tfrac{32}{27}(1-z)^3.$$

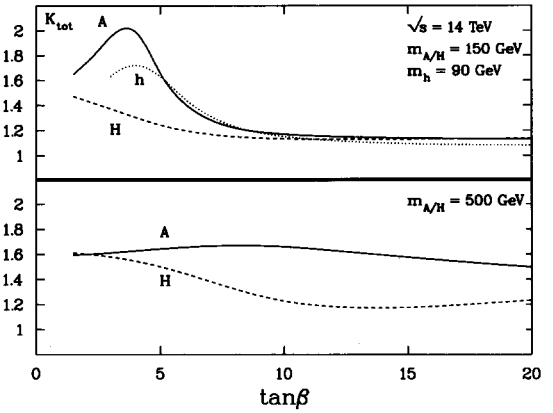

Fig. 3. The dependence of the K factors on tg β for a characteristic set of Higgs masses.

Also in the chiral limit of small quark but large Higgs masses, these coefficients approach a common limit for scalar and pseudoscalar Higgs particles.

The final results of our analysis are presented in figs. 2, 3 and 4. The on-shell quark masses have been chosen $m_b = 5$ GeV and $m_t = 140$ GeV. The cross sections have been evaluated for a set of parton distributions [13–15] that are compatible with the recent analyses of the proton structure functions at HERA [16]. The evaluation of the cross sections has been performed in the $\overline{\text{MS}}$ scheme with a Λ value $\Lambda^{(5)}_{\overline{\text{MS}}} = 131$ MeV for $N_F = 5$ quark flavors. The QCD coupling constant $\alpha_s(\mu^2)_{\overline{\text{MS}}}$ is used in next-to-leading order with the standard matching condition at $\mu = m_t$.

The K factors which characterize the size of the QCD radiative corrections properly, are defined by the ratios $K^{\Phi}_{\text{tot}} = \sigma^{\Phi}_{\text{HO}}/\sigma^{\Phi}_{\text{LO}}$. The cross sections $\sigma^{\Phi}_{\text{HO}}$ in next-to-leading order are normalized to the cross sections $\sigma^{\Phi}_{\text{LO}}$, evaluated for parton densities and α_s in leading order. K^{Φ}_{tot} split into contributions from the (regularized) virtual corrections K^{Φ}_{virt} plus the real corrections $K^{\Phi}_{ij} = \Delta\sigma^{\Phi}_{ij}/\sigma^{\Phi}_{\text{LO}}$. [Note that $K^{\Phi}_{\text{virt}} + \sum K^{\Phi}_{ij} \neq K^{\Phi}_{\text{tot}} - 1$ due to the different contributions from the subprocess (1a) to the cross sections in the LO and HO approximations.] For both the renormalization and the factorization scale $\mu = M = m_{\Phi}$ has been chosen.

The K factors can be determined in the way defined above, by adopting the GRV parametrizations of the parton densities [13] for which separate LO and HO analyses have been performed[#2]. As shown in fig. 2, K^{Φ}_{virt} and K^{Φ}_{gg} are of similar size and of order 50%, in general, while K^{Φ}_{gq} and $K^{\Phi}_{q\bar{q}}$ are quite small. Apart from the $t\bar{t}$ threshold region, the K factors K^{Φ}_{tot} are rather insensitive to the values of the Higgs masses. Near the threshold the present perturbative analysis, based on one-gluon exchange, cannot be applied anymore for the pseudoscalar particle A. In particular, since $t\bar{t}$ pairs at rest can form 0^{-+} states, the Agg coupling develops a Coulombic singularity for $m_A \approx 2m_t$. The range within a few GeV of the threshold mass must therefore be excluded from the analysis.

Outside this singular range, the QCD corrections are in general large and positive with values up to ~ 2, except for the light neutral Higgs boson h and small values of m_A for which the K factor is close to unity for large tg β. As expected, the K factor for h coincides with the corresponding SM value if m_h appoaches its maximum for a given tg β. [In this limit the MSSM reduces effectively to the SM with one light Higgs boson and SM type couplings.] The rapid change of the K factors near this limit corresponds to a rather gradual change if the SUSY space is parametrized by m_A instead of m_h. The K factors do not vary dramatically with the Higgs masses. The analytical results in the limit $\tau_Q \to 0$ provide in general a useful guideline for processes mediated by top loops. The dependence of the K factors on the parameter tg β is more pronounced, shown for a few characteristic Higgs mass values in fig. 3.

The variation of the cross sections $\sigma(pp \to h/H/A)$ in next-to-leading order, with the parton densities [13–15] is displayed in fig. 4. The rapid change of the cross section near the maximum of m_h for tg $\beta = 30$ is due to the rapid changes of the Higgs–quark couplings near this limit. This is known already from the analysis of the Higgs cross section to lowest order [2]. By singling out a small set of parametrizations, the recent results from HERA [16] have reduced the spread in the cross sections considerably, to a level of less than about 15%, so that the predictions for the

[#2] We have repeated the analysis of the K factor for Higgs production in the Standard Model based on the GRV parametrization in ref. [13]. Differences to the DFLM results in ref. [3] are very small except for very small Higgs masses.

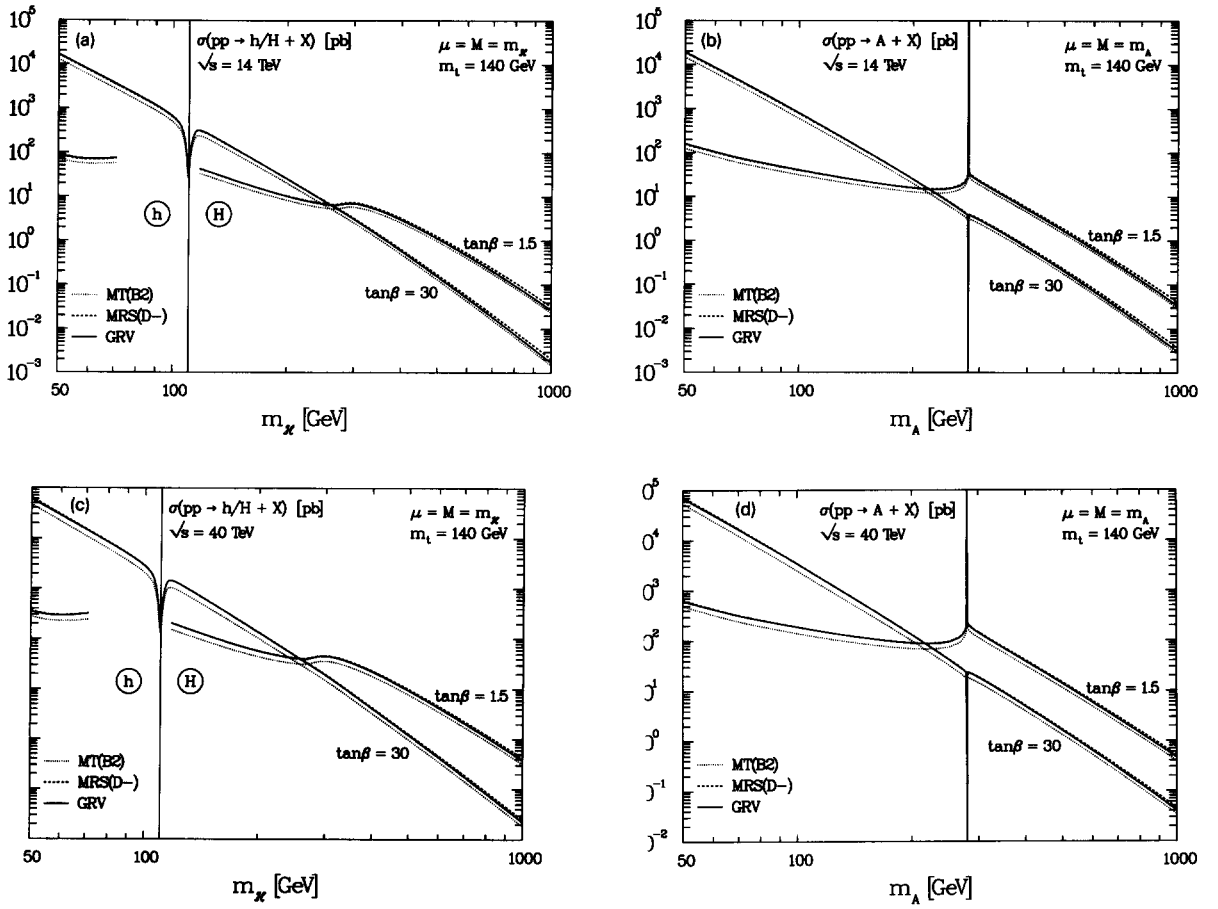

Fig. 4. The spread of the cross sections for Higgs production $\sigma(pp \to h/H/A)$ at two representative values $\mathrm{tg}\,\beta = 1.5$ and 30. Three parametrizations of the parton densities have been chosen that are compatible with the recent HERA measurements of the proton structure functions.

production of Higgs particles at pp colliders appear quite reliable.

We thank I. Hinchliffe for his critical reading of the manuscript.

References

[1] J. Gunion, H. Haber, G. Kane and S. Dawson, The Higgs Hunter's Guide (Addison-Wesley, Reading 1990).

[2] Z. Kunszt and F. Zwirner, Nucl. Phys. B 385 (1992) 3; V. Barger, M. Berger, S. Stange and R. Phillips, Phys. Rev. D 45 (1992) 4128; H. Baer, M. Bisset, C. Kao and X. Tata, Phys. Rev. D 46 (1992) 1067; J. Gunion and L. Orr, Phys. Rev. D 46 (1992) 2052.

[3] D. Graudenz, M. Spira and P.M. Zerwas, Phys. Rev. Lett. 70 (1993) 1372.

[4] A. Djouadi, M. Spira and P.M. Zerwas, Phys. Lett. B 264 (1991) 440; S. Dawson, Nucl. Phys. B 368 (1991) 283.

[5] A. Djouadi, M. Spira and P.M. Zerwas, Phys. Lett. B 311 (1993) 255.

[6] R.P. Kauffman and W. Schaffer, BNL Preprint 49061.

[7] E. Braaten and J.P. Leveille, Phys. Rev. D 22 (1980) 715; M. Drees and K. Hikasa, Phys. Lett. 240 (1990) 455; S.G. Gorishnii, A.L. Kataev and S.A. Larin, Mod. Phys. Lett. A 5 (1990) 2703.

[8] A. Djouadi, J. Kalinowski and P.M. Zerwas, Z. Phys. C 57 (1993) 569.

[9] G. 't Hooft and M. Veltman, Nucl. Phys. B 44 (1972)

189;
P. Breitenlohner and D. Maison, Comm. Math. Phys. 52 (1977) 11.
[10] S.A. Larin, Phys. Lett. B 303 (1993) 113; Preprint NIKHEF-H 92/18.
[11] G. Altarelli, R.K. Ellis and G. Martinelli, Nucl. Phys. B 157 (1979) 461;
W. Furmanski and R. Petronzio, Z. Phys. C 11 (1982) 293.
[12] This agrees with a parallel observation for the $H\gamma\gamma$ coupling; see K. Melnikov and O. Yakovlev, Phys. Lett. B 312 (1993) 179.
[13] M. Glück, E. Reya and A. Vogt, Z. Phys. C 53 (1993) 127.
[14] A.D. Martin, R.G. Roberts and W.J. Stirling, Phys. Rev. D 47 (1993) 867.
[15] J. Morfin and W.-K. Tung, Z. Phys. C 52 (1991) 13.
[16] T. Ahmed et al., Phys. Lett. B 298 (1993) 469;
M. Derrick et al., Phys. Lett. B 303 (1993) 183.